

Using Detailed Ground Modeling to Evaluate Electric Grid Impacts of Late-Time High-Altitude Electromagnetic Pulses (E3 HEMP)

Raymund H. Lee, *Student Member, IEEE*, Komal S. Shetye, *Member, IEEE*, Adam B. Birchfield, *Student Member, IEEE*, and Thomas J. Overbye, *Fellow, IEEE*

Abstract— High altitude electromagnetic pulses (HEMPs) are magnetic field fluctuations generated by nuclear bombs detonated above the earth’s surface. They have the potential to disrupt the power grid by inducing geomagnetically induced currents (GIC) on transmission lines. The magnitude of the GIC highly depends on the conductivity of the earth hundreds of thousands of meters beneath the surface. This paper describes a method to calculate HEMP electric fields using the 1D conductivity model, in which the earth is modeled with flat layers of varying thicknesses and conductivity levels. This method applies the 1D conductivity model by modifying a publicly available HEMP electric field originally calculated under the uniform conductivity model. The electric fields resulting from each model have significant differences in magnitude and locational sensitivity. A comparison of these electric fields and their impact on a power system is presented using a 10,000 bus synthetic grid.

Index Terms— Geomagnetically Induced Currents (GIC), Geomagnetic Disturbance (GMD), High Altitude Electromagnetic Pulse (HEMP), Ground Conductivity Models

I. INTRODUCTION

A nuclear bomb detonated above the earth’s surface can cause a high-altitude electromagnetic pulse (HEMP). This can create an electric field at the earth’s surface consisting of three consecutive components, called E1, E2, and E3. The E1 component occurs first, potentially having a peak magnitude measured in millions of volts per kilometer (V/km) and a duration measured in nanoseconds [1]. Next, the E2 component has a magnitude of thousands of V/km and a duration measured in microseconds. Occurring last, the E3 component can be characterized by magnitudes on the order of tens of volts per km and has a duration which is measured in seconds.

The timescale of each component determines how their effects are simulated on a power grid. The E1 and E2 components fall under the timeframe of an electromagnetic transients simulation while the E3’s timeframe is suitable for transient stability [2]. Because of this, each component is

frequently analyzed separately. This paper focuses on the E3 component.

Geomagnetic disturbances (GMDs), produce electric fields at the surface of the earth with a similar level of magnitude compared to the E3 HEMP and a time scale measured in hours [3]. GMDs occur when particles ejected from the sun reach the earth, causing its magnetic field to fluctuate.

HEMPs and GMDs both affect the power grid by inducing slowly varying, quasi-dc currents, called geomagnetically induced currents (GICs), on transmission lines. GICs impose a dc-offset on the ac currents seen by high-voltage transformers causing half-cycle saturation of the transformers’ core. This leads to the generation of harmonics, transformer heating, and an increase in the amount of reactive power absorbed by the transformer [4]. A combination of these impacts during a GMD event in 1989 resulted in a blackout of the Quebec grid, motivating the power industry to better understand GIC-related phenomena [5].

The magnitude of the electric field caused by a HEMP or GMD is highly dependent on the conductivity of the earth, hundreds of kilometers beneath the surface. The actual composition of the earth’s conductivity is very complex and different models are used to represent it. HEMP electric fields are often evaluated under a very simple model which assumes the entire earth has a single value of conductivity. This paper introduces a method which converts these electric fields under a more realistic model which is based on data from geological surveys and has regional variation. Using this method, HEMP electric fields pertaining to specific geographic areas can be calculated and the impact of a HEMP on electric grids can be evaluated with greater accuracy.

Sections of this paper are organized as follows. Section II summarizes previous work. Section III explains the method used to convert electric fields under the uniform conductivity model to the 1D conductivity model. Section IV compares the electric field magnitudes resulting from the two models using the publicly available electric field waveform from [6]. Additionally, a 10,000 bus synthetic case is used to evaluate the

This work was supported in part by the Bonneville Power Administration (BPA) under project TIP 359.

R. H. Lee, K. S. Shetye, A. B. Birchfield, and T. J. Overbye are with Texas A&M University at College Station, Texas, USA 77840.

Copyright ©2019 IEEE. Personal use of this material is permitted. However, permission to use this material for any other purposes must be obtained from the IEEE by sending a request to pubspermissions@ieee.org

(email: lee32982@tamu.edu, shetye@tamu.edu, abirchfield@tamu.edu, overbye@tamu.edu)

impact to a power grid of E3 electric fields under both conductivity models. Lastly, Section V presents a summary of the paper and introduces ideas for future research.

II. BACKGROUND

To follow the key contributions of this paper, it is helpful to review previous work about E3 HEMP electric fields and their effect on electric grids.

A. Determining the Impact of an Electric Field

If the electric field at the earth's surface is known, its impact on a power grid can be determined by first calculating the flow of induced GIC. To do this, the dc voltage induced on the transmission lines, V_{dc} , is calculated using Faraday's law [7]. The electric field, E , is integrated along the path of the transmission line using (1) where $d\bar{l}$ is the incremental length of the line.

$$V_{dc} = \oint E \cdot d\bar{l} \quad (1)$$

The dc bus voltages are then calculated using (2) where \mathbf{I} is the Norton equivalent injection currents vector calculated from V_{dc} . \mathbf{G} is the conductance matrix of the system which has been augmented to include substation grounding resistance values. \mathbf{V} is a vector containing the substation neutral dc voltages and bus dc voltages.

$$\mathbf{V} = \mathbf{G}^{-1}\mathbf{I} \quad (2)$$

With the bus voltages known, Ohm's law can be used to obtain the GIC flowing through the transmission lines and transformers. The effective GIC, $I_{GIC,pu}$, is calculated next which scales the per unit GIC flowing through each transformer depending on its winding configuration (grounded wye-delta, autotransformer, etc.).

Equation (3) is used to calculate $Q_{loss,pu}$, the reactive power absorbed by the transformer due to $I_{GIC,pu}$. K is a scaling factor which depends on the transformer's core type and number of phases and limbs. V_{pu} is the transformer's high side ac voltage in per unit [8].

$$Q_{loss,pu} = V_{pu}KI_{GIC,pu} \quad (3)$$

The base value for $Q_{loss,pu}$ is determined using (4) from [9], where $V_{high,rated}$ is the rated high-side voltage of the transformer. The base value for $I_{GIC,pu}$ is the rated high-side current of the transformer, $I_{high,rated}$.

$$Q_{base} = \sqrt{3}V_{high,rated}I_{high,rated} \quad (4)$$

The voltages across the system can be calculated by including $Q_{loss,pu}$ into the model as a constant current reactive load at the transformer buses [10].

Rise times of HEMP electric fields are on the order of seconds. To capture dynamics associated with stalling

induction motors, simulations will be performed using transient stability [11].

B. Publicly Available HEMP Electric Fields

Researchers have primarily used two publicly available HEMP electric fields to evaluate the potential impact of a HEMP on power systems [12] - [14]. In 1996, the International Electrotechnical Commission published [1] describing a time-varying electric field with no details about spatial variation. In 1985, Oak Ridge National Labs (ORNL) published [6] describing a HEMP electric field using a single time-varying waveform, which is applied to a spatially-varying contour plot shown in Fig. 1.

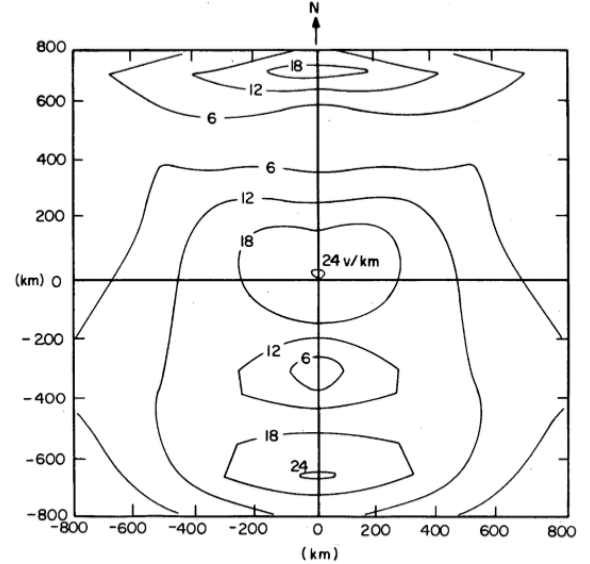


Fig. 1. The HEMP electric field's spatially-varying magnitude from [6]

A recently released report, [15], shows that the spatial variation of the actual HEMP electric field is very complex and cannot be described using a single time-varying waveform. However, because there is not enough data to fully reconstruct the actual HEMP electric field, the best practice is still to apply a single time-varying waveform to the entire HEMP footprint.

C. Ground Conductivity Models

The two publicly available electric fields mentioned, from [1] and [6], were both calculated under the uniform conductivity model which assumes the earth has a single value of conductivity. Reference [1] assumes a uniform conductivity of 10^{-4} Siemens/meter and [6] assumes 10^{-3} Siemens/meter.

Fig. 2 describes the 1D conductivity model which assumes the earth is made of flat layers of varying thicknesses and conductivity levels. This model has not been used frequently to calculate HEMP electric fields. The only known work to do this is [16], which describes a method that converts the electric field from [1] to an electric field calculated under a 2-layer 1D model.

In 2012, EPRI published [18] which partitions the United States into the 1D conductivity regions shown in Fig. 3. Each of these regions has a unique 1D conductivity profile constructed using data from geological surveys.

Because of these regionally-varying characteristics, the 1D model enables location-dependent calculations of HEMP electric fields. In later sections of this paper, the significance of this locational dependence will be described by comparing electric fields calculated under the uniform model and various 1D regions.

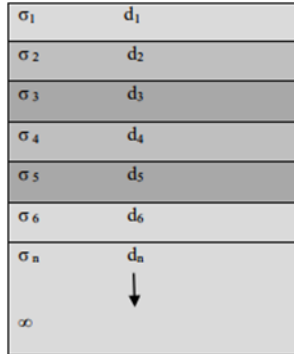


Fig. 2. 1D conductivity model description from [17]. d_n and σ_n are the depth and conductivity, respectively, of the n^{th} layer from the surface.



Fig. 3. 1D conductivity regions as shown in [18]

D. 1D Model Validity

The 1D conductivity model has been commonly used to simulate GIC induced by GMDs caused by solar activity [19] - [23]. In [22] and [23] the authors used magnetometer data collected in the field and a 1D ground conductivity model to simulate the induced GIC in the neutral of a transformer during a period of high geomagnetic activity. High correlation found between field and simulated data of these GMD events motivates the application of a 1D conductivity model to a HEMP simulation.

To build on the contributions of the work mentioned above, the next section describes how to extract the magnetic field from a uniform conductivity-based HEMP electric field, to derive electric fields using the 1D model. This approach is partly based on the method described in [17] and can be used for 1D conductivity profiles having any number of layers. Electric fields from both models will be compared in Section IV by contouring their magnitude and performing a voltage stability simulation for each model.

III. METHODOLOGY

A block diagram of the algorithm used to convert an electric

field between the uniform and 1D conductivity models is described in Fig. 4.

The electric field from [6] can be described as spatially-varying over a rectangular area of 2600 km by 2400 km. If one assumes a 25 km resolution, this can be represented by a 104 by 96 point grid. The algorithm described in Fig. 4 must be applied to every point independently to convert the entire electric field from the uniform model to the 1D model.

To help explain the algorithm, this section will include an example calculation starting with the electric field from [6], calculated under the uniform conductivity model of 10^{-3} Siemens/meter, and converting it under the ‘‘Pacific Border – 2’’ (PB-2) 1D conductivity profile, described in Fig. 5. This example will show the calculations for only one point at which the electric field has only an east-west component.

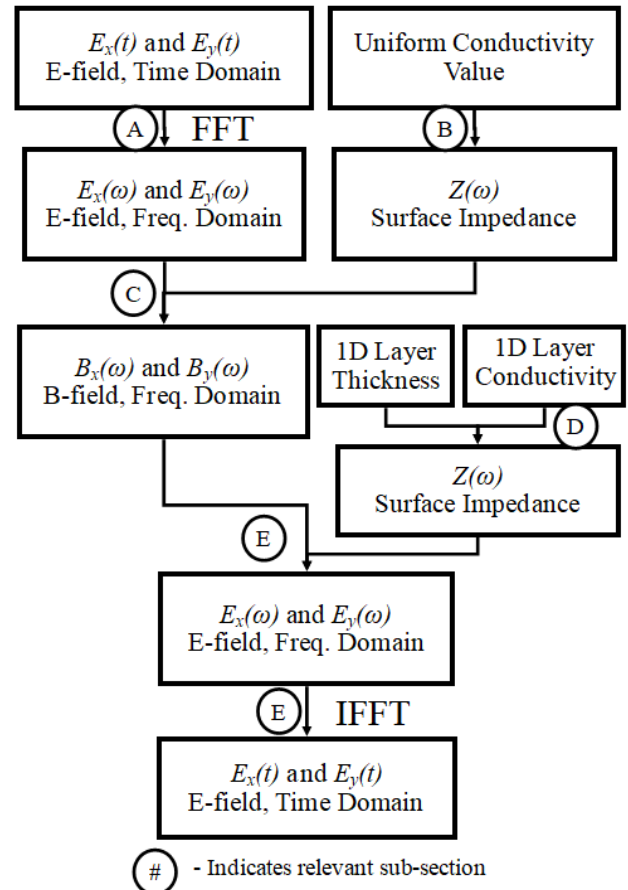


Fig. 4. High-level overview of algorithm to convert an electric field from the uniform conductivity model to the 1D conductivity model

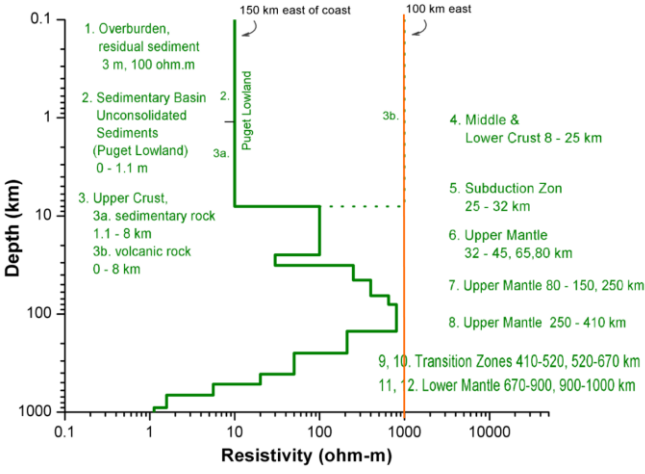


Fig. 5. 1D resistivity profile (green) vs uniform resistivity profile (orange) for region PB-2 from [17]

A. Obtaining $E(\omega)$

One of the inputs to the algorithm is the time series electric field, $E(t)$, calculated under the uniform conductivity model. As mentioned earlier, the electric field from ORNL will be used as an example during this section. The solid blue line in Fig. 6 describes its time-varying characteristics. Performing an FFT will convert the electric field from the time domain to the frequency domain as required by (5) and (6). The result of the FFT is illustrated using the solid blue line in Fig. 7. The frequencies .0089 Hz, .0445 Hz, and .0801 Hz were selected to show the results of the calculations involved in the algorithm at each step. These results are summarized in Table I.

$$E_x(\omega) = \frac{-Z(\omega)B_y(\omega)}{\mu_0} \quad (5)$$

$$E_y(\omega) = \frac{Z(\omega)B_x(\omega)}{\mu_0} \quad (6)$$

- E electric field magnitude;
- Z surface impedance;
- B magnetic flux density;
- μ_0 magnetic permeability of free space;
- x northern direction;
- y eastern direction;
- ω angular frequency;

B. Obtaining $Z(\omega)$ From Uniform Conductivity Model

The uniform conductivity model assumes that the material underneath the surface of the earth has a single value of conductivity, σ . Equation (7) is used to calculate $Z(\omega)$, using the uniform conductivity model, for each value of ω [17].

$$Z(\omega) = \frac{\sqrt{j\omega\mu_0}}{\sigma} \quad (7)$$

C. Obtaining $B(\omega)$

Knowing $E(\omega)$ and $Z(\omega)$, (5) and (6) can be used to calculate $B(\omega)$. This calculation must be performed for each value of ω [21].

D. Obtaining $Z(\omega)$ From 1D Conductivity Model

Given the depth and conductivity of each layer of the 1D ground model, the surface impedance, $Z(\omega)$, can be calculated using the method described in [17].

Each layer has a propagation constant, k_n , calculated using (8) where n is the layer number, starting with 1 as the bottom layer, and σ_n is the conductivity of the layer in Siemens/meter.

$$k_n = \sqrt{j\omega\mu_0\sigma_n} \quad (8)$$

The impedance of the bottom layer, Z_n , as seen at the surface, can be calculated using (9).

$$Z_n = \frac{j\omega\mu_0}{k_n} \quad (9)$$

To calculate the impedance of the layer above, a reflection coefficient, r_n , must be calculated using (10).

$$r_n = \frac{1 - k_n \frac{Z_{n+1}}{j\omega\mu_0}}{1 + k_n \frac{Z_{n+1}}{j\omega\mu_0}} \quad (10)$$

The impedance of the layer above, as seen at the surface, can be calculated using (11) where d_n is the thickness of the n^{th} layer.

$$Z_n = j\omega\mu_0 \left(\frac{1 - r_n e^{-2k_n d_n}}{k_n (1 + r_n e^{-2k_n d_n})} \right) \quad (11)$$

The process of using (10) and (11) must be continued iteratively for each layer until the surface of the earth is reached to get the final surface impedance value for the entire set of conductivity layers. To obtain $Z(\omega)$, this surface impedance calculation must be performed for each value of ω .

E. Obtaining $E(\omega)$ and $E(t)$ Under 1D Conductivity Model

To obtain $E(\omega)$, (5) and (6) need to be invoked again, except this time using $Z(\omega)$, calculated under the 1D conductivity model. An inverse FFT can be used to convert the electric field from the frequency domain to the time domain to obtain $E(t)$.

The orange dotted lines in Fig. 6 and Fig. 7 show the ORNL electric field, converted under the PB-2 1D conductivity profile. Comparing the two waveforms on Fig. 6, the 1D model produced a peak electric field 7.2 times smaller than the uniform model. Observing the results in rows A and E in Table I, the electric field at each frequency decreased by different amounts when converted to the 1D model. The amount of change at each frequency is dictated by the differences in $Z(\omega)$, between the uniform and 1D models, depicted in Fig. 8.

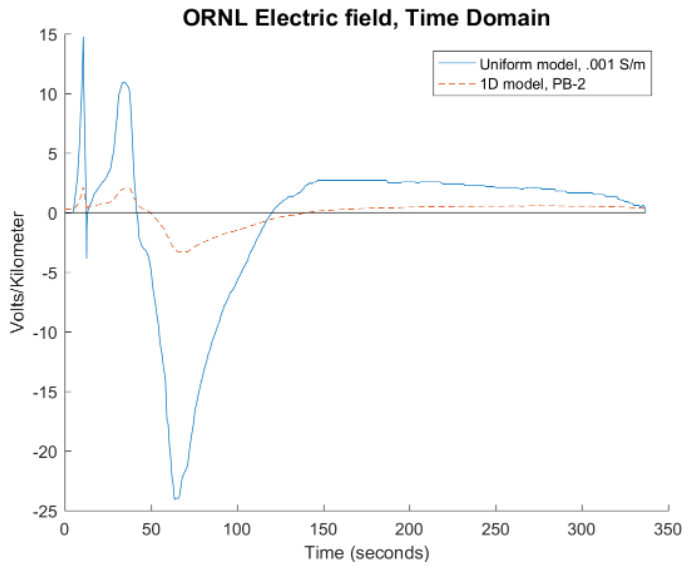


Fig. 6. ORNL electric field in the time domain.

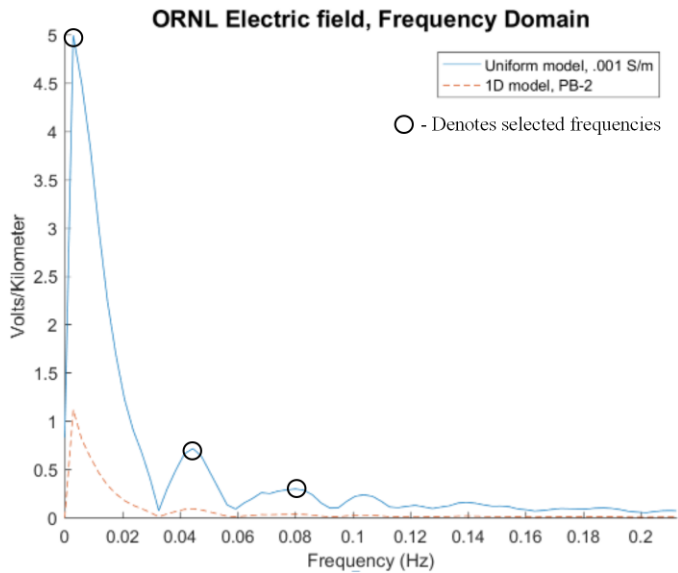


Fig. 7. ORNL electric field in the frequency domain. The circled points denote the frequencies that were selected in the example calculation.

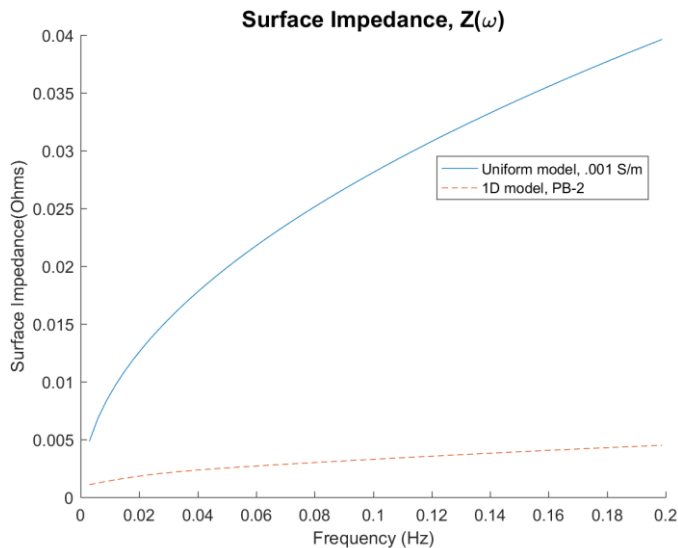


Fig. 8. Surface impedance magnitudes in the frequency domain

TABLE I
Example Calculation Results

	Frequency (Hz)	.0030	.0445	.0801
(A)	Electric Field Magnitude (Volts/km) Uniform Conductivity, .001 Siemens/meter	4.992 (-0.799+j4.93)	0.7180 (-0.697-j0.17)	0.2985 (0.0475+j0.2947)
(B)	Surface Impedance (Ohms) Uniform Conductivity, .001 Siemens/meter	0.0034 +j0.0034	0.0133 +j0.0133	0.0178 +j0.0178
(C)	Magnetic Flux Density (Teslas)	$(-8.0-j11) \cdot 10^{-4}$	$(4.1-j2.5) \cdot 10^{-5}$	$(-12.1+j8.7) \cdot 10^{-6}$
(D)	Surface Impedance (Ohms) 1D Conductivity, PB-2 Region	0.0010 +j0.0004	0.002 +j0.0013	0.0024 +j0.0017
(E)	Electric Field Magnitude (Volts/km) 1D Conductivity, PB-2 Region	1.1168 (0.264+j1.09)	0.0933 (-0.093-j0.027)	0.0356 (0.012+j0.034)

- Indicates relevant sub-section

IV. RESULTS AND ANALYSIS

This section describes the extent of how the simulated impact of the HEMP changes drastically depending on the conductivity profile used to calculate the electric field. Fig. 9 depicts the ORNL electric field under the uniform model when it is at its peak magnitude. This electric field will be converted under the 1D model at different geographic locations. Changes of electric field magnitude due to these conversions will be analyzed. To compare the impacts of these electric fields on a power system, a simulation will be performed on a synthetic grid by applying electric fields from both models.

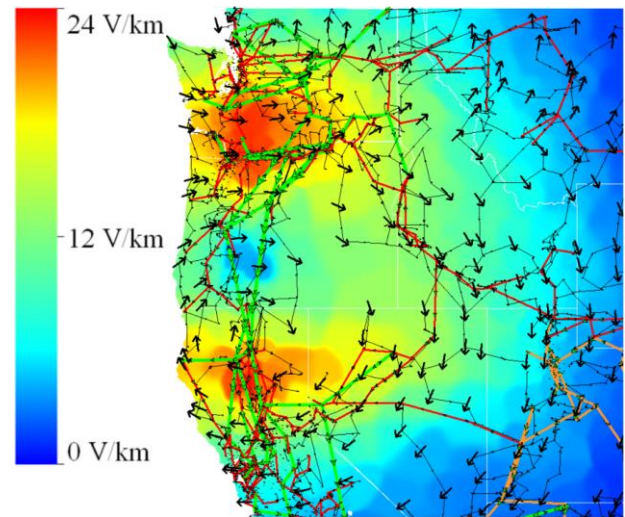


Fig. 9. Contour of ORNL electric field magnitude under a uniform conductivity model shown with the synthetic 10,000 bus system [24][25]. HEMP is centered on 45°N , -122°W . The arrows describe the electric field direction.

A. Uniform versus 1D Model - Electric Field Magnitudes

As mentioned earlier, the ORNL HEMP's geographic footprint was discretized into a 104×96 grid of points. To convert the entire electric field under the 1D model, each of these points need to be mapped to a geographic location by selecting the HEMP's center latitude and longitude. The calculations described in Section III must be done independently for each of these points. It is important to note

that the 1D conductivity region may differ from one point to another.

First, a center of 45°N , -122°W was selected. The electric field magnitudes resulting from the conversion are shown in Fig. 10.

There are significant differences between the HEMP electric field magnitudes shown in Fig. 9 and Fig. 10. These contours use the same color scale to highlight the greatly reduced electric fields in Fig. 10. These figures display the electric field magnitude when it is at its maximum intensity. In Fig. 9, the electric field shown has three distinct peaks - the top peak, middle peak, and bottom peak. The top peak has a magnitude of 19 V/km while the middle peak and bottom peak have a magnitude of 24 V/km . In contrast, in Fig. 10, the top, middle, and bottom peaks have much lower magnitudes of 3.382 V/km , 5.061 V/km , and 5.416 V/km respectively.

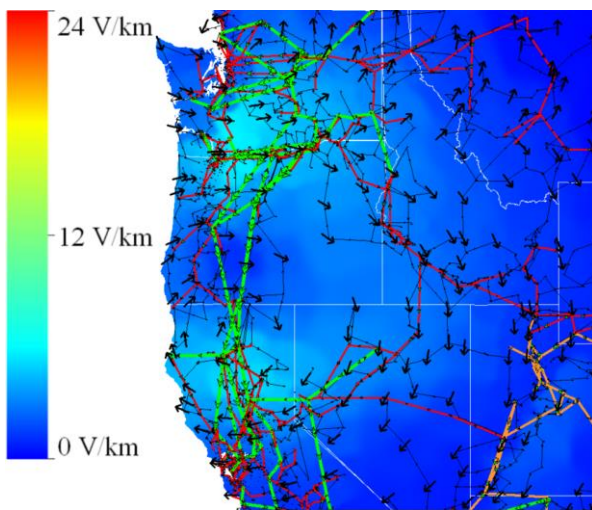


Fig. 10. Contour of ORNL electric field magnitude under a 1D conductivity model shown with the 10,000 bus system [24][25]. HEMP is centered on 45°N , -122°W . The arrows describe the electric field direction.

These differences can be explained by analyzing the resistivity profiles of each conductivity model. The 1D conductivity regions of the western United States; PB-1, PB-2, CS-1, CO-1, and BR-1; do not exceed 10^3 Ohms/meter at all depths [18]. As an example, the 1D resistivity profile of PB-2 is represented in Fig. 45 using green lines and the uniform resistivity of 10^3 Ohms/meter used by [6] is represented using an orange line. From (5) and (6), the electric field calculated under the 1D model in these western regions is expected to be weaker than one calculated with a uniform conductivity of $10^{-3}\text{ Siemens/meter}$.

The 1D model does not always yield a weaker electric field than the uniform model. Fig. 11 describes the electric field for a HEMP with a center latitude and longitude of 29°N , -97°W . In this figure, there is an abrupt change in electric field magnitude dividing the eastern and western areas of Texas. This boundary is caused by the differences in resistivity between the western and eastern conductivity regions of Texas. The southeastern region of Texas, called ‘‘Coastal Plains – 2’’ (CP-2), has a resistivity profile described in Fig. 12.

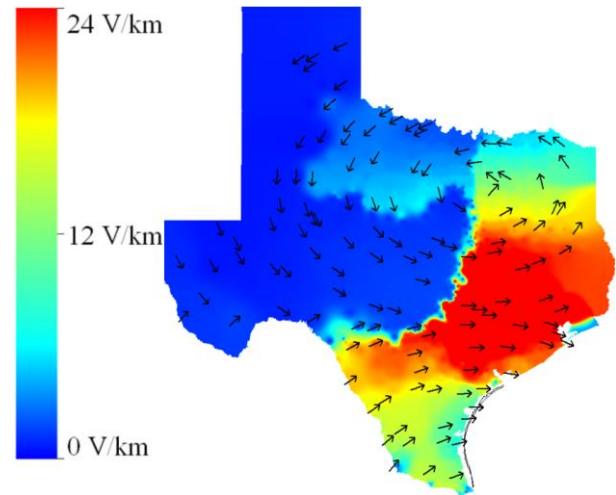


Fig. 11. ORNL electric field at its peak intensity under the 1D model. HEMP is centered on 29°N , -97°W . The arrows describe the electric field direction at each bus.

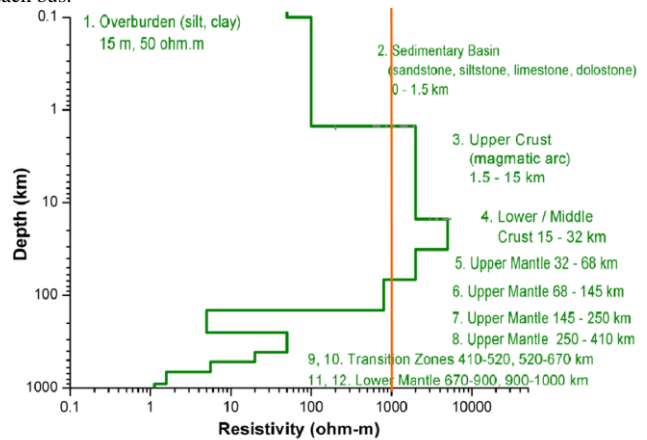


Fig. 12. 1D conductivity profile (green) vs uniform resistivity profile (orange) for region CP-2 [18]

It is not obvious whether the resulting electric field for region CP-2 is lower than the uniform model since the third, fourth, and fifth layers from the surface of the 1D model have a higher resistivity. After performing the calculations described in Section III, it was determined that region CP-2 yields a peak electric field of 31.8 V/km , which is higher than the peak electric field under the uniform model.

B. Comparing Peak Electric Field for Each 1D Region

To better understand the sensitivity of the HEMP’s electric field to location, the peak electric field of the ORNL HEMP was determined for each conductivity region published in [18]. The results of this exercise are shown on Table II. In two regions, CP-2 and PT-1, the peak electric field calculated using the 1D model was higher than the electric field calculated using a uniform conductivity of $10^{-3}\text{ Siemens/meter}$. In all other regions, the 1D model yielded a lower electric field.

TABLE II
PEAK ELECTRIC FIELD PER CONDUCTIVITY REGION FOR ORNL WAVEFORM

Conductivity Region	Max Electric Field (V/km)	Normalized to 24 V/km
IP-4	2.428	0.1012
PB-2	3.334	0.1389
IP-2	4.885	0.2035
BR-1	4.899	0.2041
CO-1	5.362	0.2234
PB-1	5.584	0.2327
CS-1	5.76	0.2400
AP-1	5.82	0.2425
SL-1	9.496	0.3957
AK-1	9.795	0.4048
CL-1	12.9	0.5375
IP-1	14.42	0.6008
IP-3	16.29	0.67875
NE-1	16.37	0.6821
AP-2	16.98	0.7075
SU-1	17.44	0.7267
CP-1	19.03	0.7929
Uniform, 10^{-3} S/m	24.0	1.000
PT-1	27.91	1.163
CP-2	31.8	1.325

The amount of variation observed between all 1D regions is significant. Comparing the two extremes of the 1D regions, region CP-2's peak electric field is over 13 times larger than region IP-4's electric field. Also, region IP-4's electric field is almost 10 times smaller than the electric field under a uniform conductivity of 10^{-3} Siemens/meter.

Electric grids can span thousands of miles and cover a geographic footprint whose conductivity varies drastically. By assuming a uniform conductivity throughout the entire footprint, an E3 HEMP simulation is subject to high levels of inaccuracy. The next subsection will illustrate how this variation affects the results of an E3 HEMP simulation on a power grid.

C. Simulations Using a Synthetic Grid

To illustrate how differently they impact an electric grid, the HEMP electric fields under the 1D and uniform models were evaluated using a 10,000 bus synthetic grid, shown on Fig. 9 and Fig. 10 [24], [25]. This fictitious grid was developed using statistical analysis of real large-scale interconnected grids and was validated against models of real systems [26].

Equation (1) was used to calculate induced dc voltages on transmission lines with the assumption that each line takes a straight path to connect two substations. To perform the integration, the lines were divided into segments 5 miles long. The electric field for each segment is assumed to be uniform and has a magnitude and direction which is interpolated by the grid of electric field data mentioned in Section A.

As mentioned in Section I, GICs affect the grid by causing transformers to saturate. Two grid impacts of GIC are evaluated in this paper: transformer hot spot heating and voltage stability due to increased reactive power absorption.

1) Transformer Hot Spot Heating

Half-cycle saturation causes magnetic flux to leak from the transformer's core, inducing eddy currents on metallic components of the transformer such as the tie-plate and the windings [27]. This results in heating and potential damage of these components [28].

NERC standard [2] requires transmission planners to perform a thermal study on transformers that exceed 75 amps per phase (A/ph) of effective GIC during a GMD simulation. Transformers that do not exceed 75 A/ph of effective GIC are considered safe from hot spot damage. The justification for using 75 A/ph as a conservative screening criterion can be found in [29].

There are 2381 transformers in the 10,000 bus synthetic grid. 103 transformers exceeded 75 A/ph of effective GIC when the HEMP under the uniform model was applied to the grid. In this scenario, the largest effective GIC magnitude seen by a transformer was 342 A/ph. This transformer stayed above 75 A/ph of effective GIC for 49.8 seconds. In contrast, when applying the HEMP under the 1D model, no transformers exceeded 75 A/ph of effective GIC. The highest levels of effective GIC flowing through transformers in each of these scenarios are described in Fig. 13.

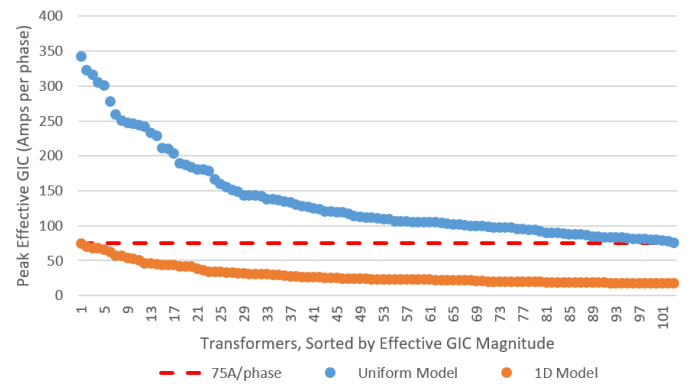


Fig. 13. Highest levels of effective GIC resulting from electric fields under the uniform and 1D conductivity models.

2) Voltage Stability Due To Reactive Power Loss

Increased reactive power absorption, leading to voltage sag, is another effect of transformer half-cycle saturation. To evaluate the voltage stability of the 10,000 bus case, a CLOD load model was used throughout the system with 25% large motors, 25% small motors, 20% discharge lighting, and 30% constant current [30].

The system-wide peak amount of reactive power absorbed by transformers due to GIC is 7,981 Mvar and 36,254 Mvar for the 1D model and uniform model, respectively. The difference in impact to the grid can be observed by comparing Fig. 14 and Fig. 15 which describe the maximum voltage deviation caused by the HEMP under each conductivity model.

Fig. 16 is a time series plot of voltage for a 345kV bus in the heavily impacted area on the west side of the 10,000 bus system. At this bus, the initial voltage started at 1.03 pu. 63.25 seconds into the simulation, the voltage dropped to 0.8386 pu and 1.0053 pu under the uniform model and 1D model respectively. The fact that there was a more extreme voltage drop under the uniform model was expected due to the

significantly faster rise-time and magnitude of reactive power absorbed by transformers under this model.

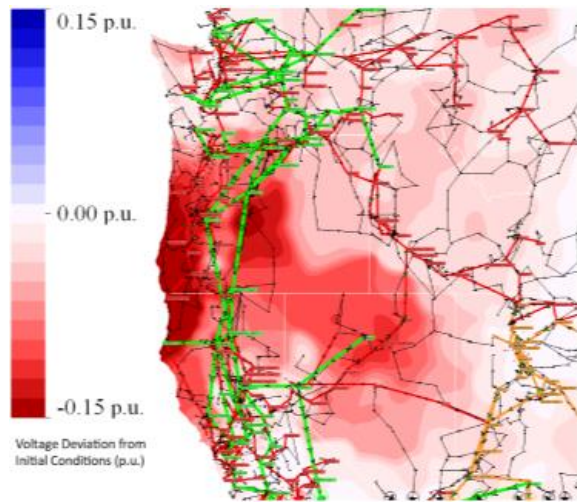


Fig. 14. Contour map showing per unit voltage deviation 63.25 seconds into the simulation (at peak intensity) with EMP under the uniform model.

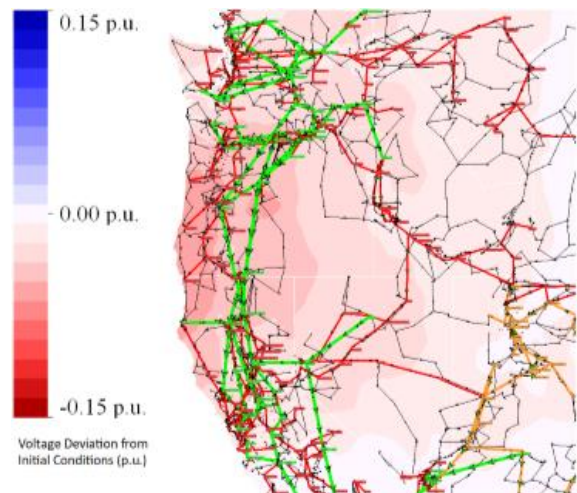


Fig. 15. Contour map showing per unit voltage deviation 63.25 seconds into the simulation (at peak intensity) with EMP under the 1D model.

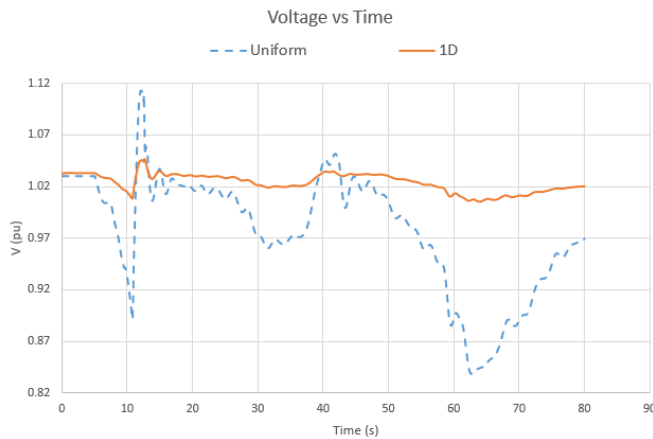


Fig. 16. Voltage fluctuations at a 345kV bus in a heavily impacted area

V. SUMMARY AND FUTURE WORK

To improve assessments of HEMP impacts on power grids, a method was introduced which converted a publicly available

electric field calculated under a simple uniform conductivity model to a more realistic 1D conductivity model. The magnitude of the electric fields resulting from the 1D conductivity model varied greatly from region to region. The uniform conductivity model does not consider these regional differences. When applying these two electric fields to a 10,000 bus synthetic case, using the 1D conductivity model yielded impacts that were much less severe.

The differences between the electric fields resulting from each model are significant. From the perspective of a power system operator, it can mean the difference between taking out transmission lines to protect system equipment and taking no action because the system appears to be safe from instability or damage.

Since the 1D model is a more realistic representation of the conductivity of the earth than the uniform model, the use of the 1D model may be preferred when performing HEMP vulnerability studies on a real system. The 1D conductivity model has been tested in multiple papers such as [22] and [23], which conclude that transformer neutral currents measured in the field have high correlation with values simulated with the 1D model.

The next step in complexity above the 1D model would be the 3D ground conductivity model like the one used in [31]. Like the 1D model, the 3D model is currently being used to evaluate GIC's induced by solar flares but has not been used to evaluate the effect of HEMPs, to the author's knowledge. For future research, it would be beneficial to compare the HEMP electric fields under 1D and 3D conductivity models.

REFERENCES

- [1] "IEC 61000-2-9 – Electromagnetic Compatibility (EMC) – Part 2: Environment – Section 9: Description of HEMP Environment – Radiated Disturbance. Basic EMC Publication," International Electrotechnical Commission. Feb. 19, 1996.
- [2] P. W. Sauer and M. A. Pai, *Power System Dynamics and Stability*, Champaign, IL: Stripes Publishing L.L.C., 1997, p. 4
- [3] "TPL-007-2 - Transmission System Planned Performance for Geomagnetic Events," National Electric Reliability Council. Nov. 2017.
- [4] J. S. Foster, E. Gjeldre, W. R. Graham, R. J. Hermann, H. M. Kluepfel, R. L. Lawson, G. K. Soper, L. L. Wood, J. B. Woodard, "Report of the Commission to Assess the Threat to the United States from Electromagnetic Pulse (EMP) Attack," EMP Commission. Apr. 2008.
- [5] "March 13, 1989 Geomagnetic Disturbance," NERC. Available: <https://www.nerc.com/files/1989-Quebec-Disturbance.pdf>
- [6] "Study to Assess the effects of Magnetohydrodynamic Electromagnetic Pulse on Electric Power System, Phase 1, Final Report," Martin Marietta Energy Systems Inc. Oak Ridge National Labs. 1985.
- [7] T. J. Overbye, T. R. Hutchins, K. S. Shetye, J. Weber, S. Dahman, "Integration of Geomagnetic Disturbance Modeling into the Power Flow: A Methodology for Large-Scale System Studies," in *Proc. 2012 North American Power Symposium*, Champaign, IL, USA, Sep. 2012.
- [8] X. Dong, Y. Liu, J.G. Kappenman, "Comparative Analysis of Exciting Current Harmonics and Reactive Power Consumption from GIC Saturated Transformers," IEEE 2001 Winter Meeting, Columbus, OH, Jan. 2001.
- [9] K. S. Shetye, T. J. Overbye, "Parametric Steady-State Voltage Stability Assessment of Power Systems using Benchmark Scenarios of Geomagnetic Disturbances," *Power and Energy Conference at Illinois*. Feb. 2015.
- [10] T. Hutchins, "Modeling, Simulation and Mitigation of the Impacts of the Late Time (E3) High-Altitude Electromagnetic Pulse on Power Systems." 2016.
- [11] T. J. Overbye, K. S. Shetye, Y. Z. Hughes and J. D. Weber, "Preliminary Consideration of Voltage Stability Impacts of Geomagnetically Induced

- Currents," in Power and Energy Society General Meeting (PES), July 2013.
- [12] G. B. Rackliffé, J. C. Crouse, J. R. Legro, V. J. Krause, "Simulation of Geomagnetic Currents Induced in a Power System by Magnetohydrodynamic Electromagnetic Pulses," Westinghouse Electric Corporation. IEEE Transactions on Power Delivery, Vol. 3, No. 1, pp. 392-397, Jan. 1988.
- [13] A.P. Sakis Meliopoulos, G. J. Cokkinides, Mario Rabinowitz, "Comparison of SS-GIC and MHD-EMP-GIC Effects on Power Systems," IEEE Transactions on Power Delivery, Vol 9, No. 1, pp. 194-207, Jan. 1994.
- [14] R. Horton, "Magnetohydrodynamic Electromagnetic Pulse Assessment of the Continental U.S. Electric Grid," Electric Power Research Institute. Feb. 2017.
- [15] "Recommended E3 HEMP Heave Electric Field Waveform for the Critical Infrastructures," United States EMP Commission. Volume II. Jul. 2017.
- [16] J. Gilbert, J. Kappenman, W. Radasky, E. Savage, "The Late-Time (E3) High-Altitude Electromagnetic Pulse (HEMP) and Its Impact on the U.S. Power Grid," Oak Ridge National Laboratory, Metatech Corporation, Jan. 2010.
- [17] "Application Guide: Computing Geomagnetically-Induced Current in the Bulk-Power System, " NERC, Dec. 2013. [Online]. Available: <http://www.nerc.com/comm/PC/Geomagnetic%20Disturbance%20Task%20Force%20GMDTF%202013/GIC%20Application%20Guide%20013-approved.pdf>
- [18] P. Fernberg, "One-Dimensional Earth Resistivity Models for Selected Areas of Continental United States & Alaska," EPRI, Palo Alto, CA, Technical Results (1026430), 2012.
- [19] L. Marti, C. Yiu, A. Rezaei-Zare, D. Boteler, "Simulation of Geomagnetically Induced Currents With Piecewise Layered-Earth Models," IEEE Transactions on Power Delivery, Vol 29, No. 4, pp. 1886-1893, Aug. 2014.
- [20] K. Zheng, L. Trichtchenko, R. Pirjola, L. Liu, "Effects of Geophysical Parameters on GIC Illustrated by Benchmark Network Modeling," IEEE Transactions on Power Delivery, Vol 28, No. 2, pp. 1183-1191, Apr. 2013.
- [21] D.H. Boteler, "Geomagnetically Induced Currents: Present Knowledge and Future Research" IEEE Transactions on Power Delivery, Vol 9, No. 1, pp. 50-58, Jan. 1994.
- [22] T. Halbedl, R. Bailey, G. Achleitner, H. Renner, R. Leonhardt, "Analysis of the Impact of Geomagnetic Disturbances on the Austrian Transmission Grid." Power Systems Computation Conference. Dec. 2016.
- [23] A. Pulkkinen, R. Pirjola, A. Viljanen. "Determination of Ground Conductivity and System Parameters for Modeling of Geomagnetically Induced Current Flow in Technological Systems." Sept. 2007.
- [24] A. B. Birchfield, T. Xu, K.M. Gegner, K.S. Shetye, T.J. Overbye, " Grid Structural Characteristics as Validation Criteria for Synthetic Networks," IEEE Transactions on Power Systems, vol. 32, no. 4, pp. 3258-3265, Jul. 2017.
- [25] T. Xu, A. B. Birchfield, T. J. Overbye, "Modeling, tuning, and validating system dynamics in synthetic electric grids," IEEE Transactions on Power Systems, to appear, 2018.
- [26] A. B. Birchfield, E. Schweitzer, M.H. Athari, T. Xu, T. J. Overbye, A. Scaglione, Z. Wang, "A metric-based validation process to assess the realism of synthetic power grids," Energies, vol. 10, no. 1233, pp. 1-14, Aug. 2017.
- [27] L. Marti, A. Rezaei-Zare, A. Narang, "Simulation of Transformer Hotspot Heating due to Geomagnetically Induced Currents," IEEE Transactions on Power Delivery, vol. 28, no. 1, Jan. 2013.
- [28] "Transformer Thermal Impact Assessment White Paper," North American Electric Reliability Corporation. Dec. 2014.
- [29] "Screening Criterion for Transformer Thermal Impact Assessment," North American Electric Reliability Corporation. May. 2016.
- [30] "Load Characteristic CLOD Complex Load Model," Available: https://www.powerworld.com/WebHelp/Content/TransientModels_HTML/Load%20Characteristic%20CLOD.htm
- [31] J.L. Gannon, A. B. Birchfield, K. S. Shetye, T. J. Overbye, "A Comparison of Peak Electric Fields and GICs in the Pacific Northwest Using 1-D and 3-D Conductivity," Space Weather Journal, Oct. 2017.

Raymund H. Lee (S'17) received the B.S. degree in Electrical and Computer Engineering in 2013 from The University of Texas, Austin, TX, USA. He is now pursuing an M.S. degree in Electrical and Computer Engineering at Texas A&M University, College Station, TX, USA.

Komal S. Shetye (S'10–M'11) received the B. Tech (2009) and MSEE (2011) degrees in Electrical Engineering from the University of Mumbai, India and the University of Illinois at Urbana-Champaign, IL, USA, respectively. She is currently an Associate Research Engineer – Faculty in the Texas Engineering experiment Station (TEES) and the Department of Electrical Engineering at Texas A&M University, College Station, TX, USA.

Adam B. Birchfield (S'13) received the B.E.E. degree in 2014 from Auburn University, Auburn, AL, USA, and the M.S. degree in Electrical and Computer Engineering in 2016 from the University of Illinois at Urbana-Champaign, Urbana, IL, USA. He is now a Ph.D. candidate in electrical engineering at Texas A&M University, College Station, TX, USA.

Thomas J. Overbye (S'87–M'92–SM'96–F'05) received the B.S., M.S., and Ph.D. degrees in electrical engineering from the University of Wisconsin-Madison, Madison, WI, USA. He is currently a TEES distinguished research Professor in the Department of Electrical and Computer Engineering at Texas A&M University, College Station, TX, USA.